Experimental Thermal and Fluid Science 91 (2018) 144–154

Contents lists available at ScienceDirect

Experimental Thermal and Fluid Science

journal homepage: www.elsevier.com/locate/etfs

Measuring radiative properties of silica aerogel composite from FTIR transmittance test using KBr as diluents

Hu Zhang*, Xian Wang, Yueming Li

State Key Laboratory for Strength and Vibration of Mechanical Structures, Shaanxi Key Laboratory of Environment and Control for Flight Vehicle, School of Aerospace, Xi'an Jiaotong University, Xi'an, Shaanxi 710049, PR China

ARTICLE INFO

Keywords:
Extinction coefficient
Radiative thermal conductivity
Silica aerogel composite
KBr diluents
Fourier transform infrared spectroscopy

ABSTRACT

Radiative properties such as spectral extinction coefficient, Rosseland mean extinction coefficient and radiative thermal conductivity are the key features of porous insulation materials. For silica aerogel composites with fiber and opacifier, it is difficult to determine the spectral extinction coefficient and radiative thermal conductivity via experiment accurately. The spectral extinction coefficient of such composites is usually determined by a transmittance test using KBr as a diluent. The traditional model has several assumptions on determining the extinction coefficient from the transmittance measurement: the diluents are assumed as a pure transparent medium, the pressed pellet has no reflection, and the composite powder is in series with the KBr when calculating the effective thickness of the composite. Thus, the extinction coefficient determined from the traditional model with these assumptions will result in some uncertainty on predicting the radiative thermal conductivity. To overcome the drawbacks, improved models are proposed by considering the absorption of KBr diluents, sample reflection and random distribution of sample powder in the diluents. KBr diluted silica aerogel composite pellets with the same constituents and concentrations but different thicknesses are prepared using the pressed pellets method. The transmittances of the pressed pellets are measured by Fourier transform infrared spectroscopy (FTIR). The spectral extinction coefficients are calculated from the measured transmittances with proposed models. The radiative thermal conductivity of silica aerogel composite is calculated with the measured Rosseland mean extinction coefficient determined from different models. This study found that the developed models could eliminate the assumptions of the traditional model.

1. Introduction

Materials with high porosity are typically applied as thermal insulation materials. Heat transfer within porous materials occurs via three modes: conduction, convection and radiation. Thermal radiation of high porous materials will become a prominent or even dominant heat transfer mode at high temperature. Therefore, theoretical and experimental studies have been focused on revealing the radiative properties and reducing thermal radiation of porous materials [1–5]. The capacity of materials to attenuate thermal radiation can be described by the spectral extinction coefficient, which is composed of spectral absorption coefficient and spectral scattering coefficient. The spectral extinction coefficient needs to be determined prior to the calculation of other radiative properties, such as Rosseland mean extinction coefficient and radiative thermal conductivity (λ_r). Extinction coefficient test has also been widely conducted to analyze other related properties such as the mechanism of soot formation and growth in combustion systems, the optimization of the photothermal conversion efficiency of nanorods, and nanoparticles in biomedicine and energy conversion [6–8].

Silica aerogel is a typical nano-porous material with high thermal insulation performance. The nano-sized pores and skeleton are responsible for the low thermal conductivity of aerogel. However, pure silica aerogel with high porosity is fragile and nearly transparent in the spectral range from 3 to 8 μm at temperatures less than 1000 K [9]. Thus, reinforced fiber and opacifier are usually doped in silica aerogel to enhance its mechanical strength and the extinction of thermal radiation at high temperature. It is necessary to know the spectral extinction coefficient of such composites to optimize their temperature dependent thermal insulation performance. Many studies have been conducted to predict and measure the effective thermal conductivity of silica aerogel composites [9–21]. However, until now there have very few experiment data of spectral extinction coefficient of fiber and opacifier loaded silica aerogel.

The existence of strong absorption peaks near 9 μm and 21 μm makes it difficult to measure the spectral extinction of silica aerogel

* Corresponding author.
E-mail address: huzhang@xjtu.edu.cn (H. Zhang).

http://dx.doi.org/10.1016/j.expthermflusci.2017.10.010
Received 7 June 2017; Received in revised form 4 September 2017; Accepted 10 October 2017
Available online 16 October 2017
0894-1777/

because it is difficult to prepare a sample thin enough to transmit infrared beam near these wavelengths. Thinner specimens are required for the transmittance measurement of silica aerogel with high density or composite with fiber and opacifier. Several methods have been developed to overcome the difficulty of obtaining thin samples for FTIR test [22–26]. One method is grinding the aerogel into powder and then placing it between two infrared transparent plates. Although this method does not involve other material components, the porosity will be changed after pressing and it will be difficult to determine its apparent density. The mineral oil mull method was also used to mix aerogel which is then spread onto a thin infrared polyethylene foil [23]. Zeng et al. used fine sand paper to grind aerogel to a 30 μm thick sample [22]. Zhao also prepared aerogel samples with thicknesses between 1 mm and 11 mm using sand paper [24]. Fu et al. prepared fiber loaded silica aerogel composites with different thicknesses directly using sol-gel and the supercritical drying technique for scattering and absorption coefficient measurements [25]. Cohen and Glicksman manufactured monolithic aerogel with thickness between 0.1 mm and 1 mm for extinction coefficient measurements [26]. Diluents, such as KBr which is nearly transparent to infrared radiation, are also widely used to dilute materials in the transmittance measurement for its convenience and large transparent spectral region [3,27,28].

Although the structures of silica aerogel samples prepared for transmittance measurements can be the same after grinding with sand paper, it is rather difficult to grind a sample thin and smooth enough, especially for these fragile materials. It is also inconvenient and expensive to obtain infrared test samples via manufacturing the sample directly. Adopting diluents to prepare infrared test samples by pressed pellets method is one more general method. In this method, the diluents are assumed transparent without any absorption or scattering and there is no reflection on the sample surface. The equivalent thickness of the test sample powder in the KBr diluents corresponding to the materials before grinding is calculated by assuming KBr is in series with the test sample. The assumptions of KBr diluted pressed pellets method may bring some uncertainty in the determination of the extinction coefficient.

In the present study, the models of determining extinction coefficient using KBr diluted pressed pellets method will be improved by taking account of the practical transparency of KBr diluents, the reflection on the sample surface and the practical distribution of the sample powder in the KBr diluents. The transmittance of fiber and opacifier loaded silica aerogel with different concentrations will be measured by FTIR using KBr diluted pressed method. The spectral extinction coefficient will then be determined from the proposed models. Finally, the radiative thermal conductivity of the silica aerogel composite is calculated from the Rosseland model with the measured extinction coefficient.

2. Models of extracting extinction coefficient from FTIR transmittance test

2.1. Traditional model: model 1

The schematic diagram of the radiation intensities balance of an FTIR measurement is shown in Fig. 1. A collimated beam with intensity of I_L irradiates the pellet, part of the intensity (I_R) is reflected back by the pellet and the rest (I_0) enters the pellet. The radiation within the pellet will be attenuated by absorbing and scattering. The intensity attenuated by the pellet is denoted by I_A. Finally, only the intensity I_T is transmitted by the pellet.

From an FTIR measurement, the spectral extinction coefficient can be calculated from the measured spectral transmittance using

$$\tau_\lambda = \frac{I_T}{I_0} \approx \frac{I_T}{I_L} = \exp(-k_\lambda L) \tag{1}$$

where τ_λ is the transmittance of pellet, L is the sample thickness and k_λ is the spectral extinction coefficient. The beam intensity irradiates on the pellet is not identical to the intensity enters the pellet due to the surface reflection. In Eq. (1), the reflection by the pellet is usually neglected for simplification due to the high transparency of KBr.

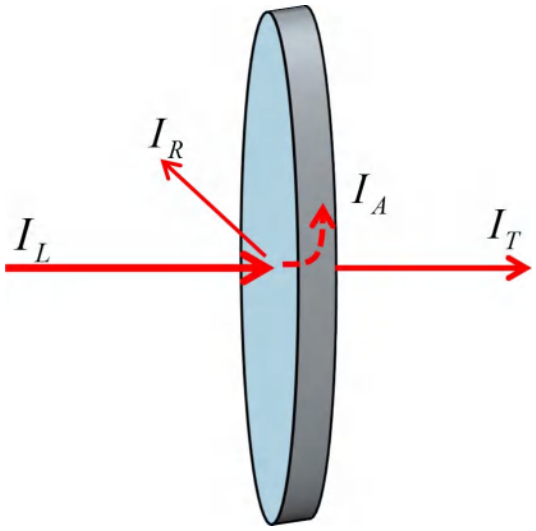

Fig. 1. Schematic diagram of beam intensities in FTIR transmittance test.

For KBr diluted pellet, KBr is assumed transparent to the infrared beam. The effective thickness of the diluted material is determined by

$$L_c = \frac{W \cdot P}{\rho A} \tag{2}$$

where W is the weight of the pellet, P is the mass ratio of the test material in the pellet, ρ is the density of the test material and A is the cross-sectional area of the pellet. In this equation, the equivalent thickness is calculated by assuming the test sample occupies the full cross section area as shown at the upper part of Fig. 2. Combine Eqs. (1) with (2), the spectral extinction coefficient (k_λ) can be calculated from [7]

$$k_\lambda = -\ln\tau_\lambda / L_c \tag{3}$$

In this model, KBr is transparent, the pellet has no reflection, and the test material occupies the full cross section area. This model is essentially a series model of KBr and test material along the beam direction. In fact, KBr is not absolute transparent to infrared beam, especially when exposed in air. The transparency of KBr will decrease after adsorbed water vapor or carbon dioxide. The test material mixed with KBr is more like randomly distributed in KBr as shown at the lower part of Fig. 2. Therefore, the equivalent thickness of test material

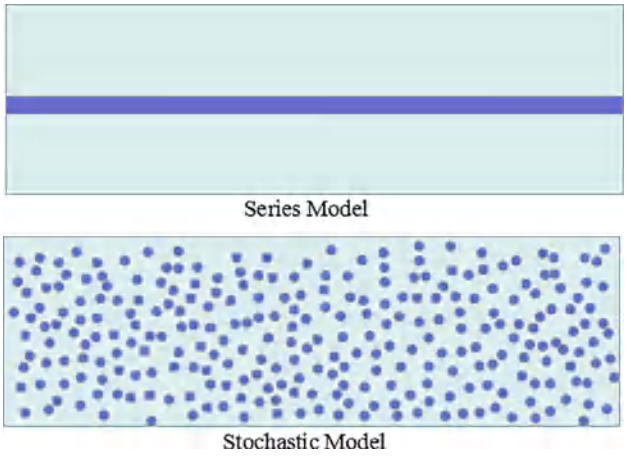

Fig. 2. Schematic diagram of series model and stochastic model.

Table 1
Model assumptions.

Models	Assumptions
Model 1	Neglecting surface reflection; neglecting absorption of KBr; series model: sample powder occupied the full cross section area
Model 2	Neglecting surface reflection; considering absorption of KBr; series model
Model 3	Considering surface reflection; considering absorption of KBr; series model
Model 4	Considering surface reflection; considering absorption of KBr; stochastic model: sample is randomly distributed in the KBr diluents

determined by Eq. (2) will be underestimated and result in an overestimated extinction coefficient. In addition, the neglecting of surface reflection will increase the uncertainty. In the next subsection, models are developed by considering the practical transparency of KBr, the distribution of test materials in KBr diluents, and the reflection of the pellet surface.

2.2. Improved models

To overcome the deficiencies of traditional model, three improved models are developed in this subsection. The comparisons of the four models are listed in Table 1. Compared with traditional model, the absorption of KBr is considered in Models 2, 3 and 4, the sample surface reflection is taken into account in Models 3 and 4 while the random distribution of test materials is considered in Model 4.

2.2.1. Model 2: considering the absorption of KBr

The practical transparency of KBr can be revealed by conduction a separate FTIR transmittance test. Then the spectral extinction coefficient of test material can be calculated from

$$\tau_\lambda = \frac{I_T}{I_0} \approx \frac{I_T}{I_L} = \exp(-k_\lambda L_c - k_{KBr} L_{KBr}) \tag{4}$$

where k_{KBr} is the spectral extinction coefficient of KBr, $L_{KBr} = L - L_C$ is the equivalent thickness of KBr. Compared with Model 1, Model 2 considers the practical transparency of KBr.

2.2.2. Model 3: considering the surface reflection

The beam intensities irradiate on the sample and transmitted by the sample can be measured by conducting measurements with and without the sample (as a control). Due to the surface reflecting, the beam intensity entering the pellet cannot be obtained directly, thus the right side of Eq. (4) can be described in form of

$$\frac{I_T}{I_L} = \frac{I_0}{I_L}\frac{I_T}{I_0} = \left(1 - \frac{I_R}{I_L}\right)\exp(-k_\lambda L_c - k_{KBr} L_{KBr}) \tag{5}$$

By measuring the intensity irradiated on the pellet and the beam intensity transmitted via pellets of different thickness, a series of $I_T/I_L \sim L_c$ can be obtained. Then the spectral extinction coefficient of test material with considering surface reflection and absorption of KBr can be calculated from

$$\ln\left(\frac{I_T}{I_L}\right) = \ln\left(1 - \frac{I_R}{I_L}\right) - k_\lambda L_c - k_{KBr} L_{KBr} \tag{6}$$

In Eq. (6), the pellets with different thickness are prepared with the same material, the same concentration, and the same grinding mortar, thus the reflection (I_R/I_L) of different thickness pellets can be regarded as a constant. With the values of $I_T/I_L \sim L_c$, the spectral extinction coefficient of test material can be obtained from the slope of the fitted linear relation of $\ln(I_T/I_L) \sim L_c$. This fitting method is proposed by Cohen and Glicksman to eliminate the influence of surface reflectance [26].

2.2.3. Model 4: considering stochastic distribution of test sample

In the above three models, the test material is assumed in series with KBr when calculating the equivalent thicknesses of test material and diluted KBr. In practice, the test material is more like randomly distributed in KBr as shown at the lower part of Fig. 2. In this section, a stochastic model is proposed. When the beam is transmitted through a short distance (ΔL) along the through-plane direction of test pellet, the transmittance is

$$\frac{I_{T'}}{I_{0'}} = \phi\exp(-k_\lambda \Delta L) + (1-\phi)\exp(-k_{KBr}\Delta L) \tag{7}$$

here ϕ is the area fraction of test sample in the pellet while $(1-\phi)$ is the area fraction of KBr. For an arbitrary cross section, the area fraction of the test sample is identical to its volume fraction by assuming each cross-section area has the same area proportion. For pellets with m layers in series, the overall transmittance is

$$\frac{I_T}{I_0} = \frac{I_{T^1}}{I_0}\frac{I_{T^2}}{I_{T^1}}\cdots\frac{I_{T'}}{I_{T^{m-1}}} = [\phi\exp(-k_\lambda \Delta L) + (1-\phi)\exp(-k_{KBr}\Delta L)]^m \tag{8}$$

where $\Delta L = L/m$.

Substitute Eq. (8) into Eq. (5), the influence of reflecting can be considered by

$$\frac{I_T}{I_L} = \frac{I_0}{I_L}[\phi\exp(-k_\lambda \Delta L) + (1-\phi)\exp(-k_{KBr}\Delta L)]^m \tag{9}$$

Similar to Eq. (6), taking the logarithm of Eq. (9) leaves

$$\begin{aligned}\ln\left(\frac{I_T}{I_L}\right) &= \ln\left(\frac{I_0}{I_L}\right) + m\ln[\phi\exp(-k_\lambda \Delta L) + (1-\phi)\exp(-k_{KBr}\Delta L)] \\ &= \ln\left(1 - \frac{I_R}{I_L}\right) + m\ln[\phi\exp(-k_\lambda \Delta L) + (1-\phi)\exp(-k_{KBr}\Delta L)] \\ &= \ln\left(1 - \frac{I_R}{I_L}\right) + \overline{k_\lambda} L\end{aligned} \tag{10}$$

where $\overline{k_\lambda} = \ln[\phi\exp(-k_\lambda \Delta L) + (1-\phi)\exp(-k_{KBr}\Delta L)]/\Delta L$ represents the effective spectral extinction coefficient of each layer. With a series of measured $I_T/I_L \sim L$, $\overline{k_\lambda}$ and k_λ can be obtained.

2.3. Radiative thermal conductivity

The radiative thermal conductivity of an optical thick medium can be predicted by the Rosseland model [29]:

$$\lambda_r = \frac{16}{3K_{e,m}}\sigma n^2 T^3 \tag{11}$$

where n is the materials' effective refractive index, σ is the Stefan-Boltzmann constant, T is the mean temperature, and $K_{e,m}$ is Rosseland mean extinction coefficient which is defined as

$$\frac{1}{K_{e,m}} = \frac{\int_0^\infty \frac{1}{k_\lambda}\frac{\partial e_{b\lambda}}{\partial T}d\lambda}{\int_0^\infty \frac{\partial e_b}{\partial T}d\lambda} = \int_0^\infty \frac{1}{k_\lambda}\frac{\partial e_{b\lambda}}{\partial e_b}d\lambda \tag{12}$$

where $e_{b\lambda}$ is the spectral hemispherical blackbody flux and e_b is the hemispherical blackbody flux.

Because the distance of mirror motion in FTIR system is not infinitely long, the test wavelength range of FTIR instrument is finite. Thus, the wavelength range of integral is finite and identical to the experimental range. The range of integral of Eq. (12) is modified as follows.

$$\frac{1}{K_{e,m}} = \int_{\lambda_1}^{\lambda_2} \frac{1}{k_\lambda}\frac{\partial e_\lambda}{\partial e_b}d\lambda \tag{13}$$

For aerogel composite loaded with fiber and opacifier, its effective refractive index can be calculated by [4]:

$$n = V_f n_f + V_{opa} n_{opa} + V_a n_a \tag{14}$$

Table 2
Sample properties.

Sample	Density (kg/m^3)	Porosity (%)	Volume fraction (matrix: fiber: opacifier)	Mass fraction (matrix: fiber: opacifier)	Effective refractive index
A	346.4	83.4	99.49:0.51:0	96.99:3.01:0	1.12
B	368.1	85.2	97.32:0.51:2.17	78.93:2.82:18.26	1.14
C	387.1	86.7	95.74:0.51:3.75	67.11:2.69:30.2	1.16

where V_f,V_{opa},V_a and n_f,n_{opa},n_a are the volume fractions and effective refractive indexes of fiber, opacifier and aerogel, respectively. The refractive index of silica aerogel is determined by

$$n_a = V_s n_s + V_g n_g \tag{15}$$

where n_s and n_g are the refractive indexes of bulk silica and gas within pores and V_s and V_g are the volume fractions of silica skeleton and gas of aerogel matrix.

3. Samples preparation and measurements

3.1. Material information

Radiative properties of three silica aerogel samples loaded with different contents of fiber and opacifier (as listed in Table 2) are studied. The composite materials are constituted of a SiO_2 matrix, SiO_2 fiber with diameter of 6 μm and SiC opacifier with mean diameter of 3.5 μm. The effective refractive index is calculated from Eqs. (14) and (15). In the calculation, the refractive indexes of bulk silica and SiC opacifier are set as 1.58 and 2.67, respectively [12,22].

3.2. Experimental procedures

KBr with purity higher than 99.9% is used as the diluent. When conducting the transmittance measurements, there are three important experimental procedures to follow.

(1) Drying the material: KBr diluents and aerogel composite are dried for 12 h at 110 °C to remove the adsorbed water before pressing the pellet.
(2) Pressing the pellet: Aerogel composite is diluted about 200 times in weight as shown in Table 3. KBr and silica aerogel composite are mixed and ground in an agate mortar for 3–5 minutes to obtain fine powders. The mixed powders are pressed by a Tablet Press Machine at 12 MPa for 2 minutes. Thin circular pellets with diameter of 13 mm are manufactured after pressing. For each sample, several pellets are prepared with the same concentration but different thickness as listed in Table 3.
(3) Transmittance measurement: The spectrum of the light source is measured by FTIR without placing any sample in the optical path and stored as background for reference. Transmittances of KBr pellets and KBr diluted aerogel composite pellets are measured by comparing the transmitted spectrum with the reference spectrum. Compensation of water vapor and carbon dioxide is made by the instrument software OPUS. For each spectrum, 32 scans are made and the average is taken. The scan is made within 400–7500 cm^{-1} (1.33–25 μm) with a scan interval of 2 cm^{-1}.

Table 3
Parameters of pellets.

Materials	Mass ratio of composite and KBr	Thickness of pellet (mm)			
		Pellet 1	Pellet 2	Pellet 3	Pellet 4
A	1:122	0.403	0.556	0.670	–
B	1:178	0.546	0.560	0.839	0.853
C	1:202	0.415	0.536	0.619	0.791

3.3. Instruments

The mass is measured by an electric balance with repeatability of 0.1 mg (XP404S, METTLER TOLEDO) and the thickness is measured by a micrometer with an accuracy of 10 μm. The transmittance is measured by FTIR spectroscopy (VERTEX70, BRUKER). The FTIR spectroscopy has a built-in optical modification to modulate the light source to a collimated beam. In the FTIR test, FTIR utilizes collimated light and Michelson interferometer to obtain an interferogram. Fourier transform algorithm is adopted to calculate the reflected or transmitted spectrum.

4. Results and discussion

4.1. Transmittance and spectral extinction coefficient of KBr

KBr is not completely transparent to near-infrared and mid-infrared radiation and will easily adsorb water vapor and carbon dioxide from the atmosphere. To exclude the absorption of KBr, the spectral extinction coefficients of KBr are measured by pressing KBr pellets. Fig. 3 shows the transmittances of KBr pellets with different thickness (marked in the figure). Due to the adsorption of water vapor, the transmittances of KBr pellets measured after the FTIR experiment are decreased at full wavelength range.

The spectral extinction coefficients of KBr shown in Fig. 4 are calculated from Eq. (3). Reflectance of the KBr pellet is neglected when determining its extinction coefficient from Eq. (1) because KBr has very high transmittance. In Figs. 3 and 4, three absorption peaks at 2.9 μm, 6.1 μm and 9.1 μm are clearly observed which are caused by the vibration of hydroxyl of residual water. Although the KBr diluent is dried before pressing pellets, little water is still existed in the KBr powder. In addition, KBr diluent will adsorb water vapor when stored in air which can be seen from the increased absorption peaks after finishing the FTIR test. The spectral extinction coefficients of KBr diluents are on the order of several cm^{-1} and mainly within 1.5–2.5 cm^{-1}. The spectral extinction coefficients of KBr obtained from KBr pellets of different thickness are averaged and treated as the extinction coefficient of KBr in the following analysis.

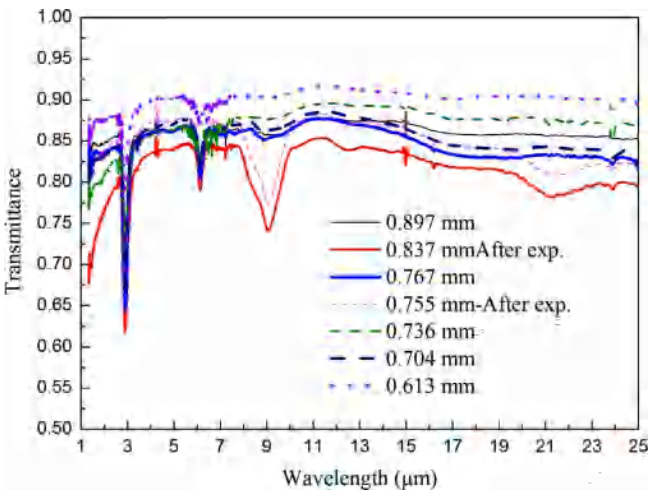

Fig. 3. Transmittance of KBr.

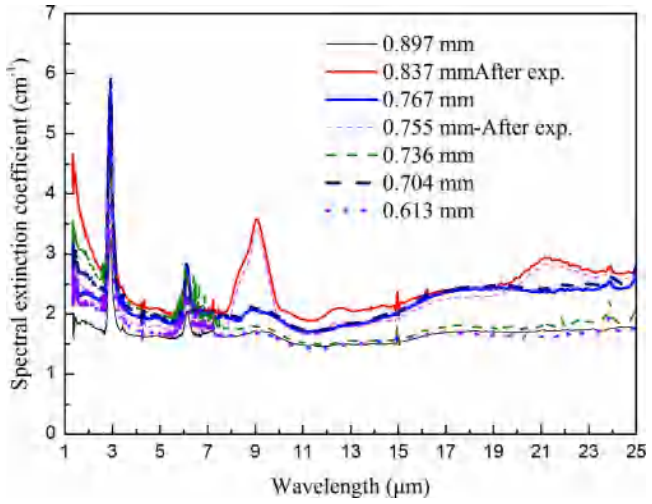

Fig. 4. Spectral extinction coefficient of KBr.

4.2. Transmittance of KBr diluted silica aerogel composite

The transmittances of three KBr diluted aerogel composite measured by FTIR are shown in Fig. 5. The transmittances of these samples have the same spectral dependency. Despite the absorption peaks of water at 2.9 μm, 6.1 μm and 9.1 μm, peaks are also observed at 10.5 μm, 12.3 μm and 21.2 μm, which agree well with the standard infrared spectrum of SiO_2 aerogel [30,31].

4.3. Spectral extinction coefficient of silica aerogel composite

With the measured transmittance, the spectral extinction coefficients of aerogel composites can be calculated by the models in Section 2 which are summarized in Table 1. The traditional model assumes no sample surface reflection, no absorption of KBr, and aerogel powder occupies full cross-sectional area. The improved models are developed by taking into account the practical surface reflection, absorption of KBr, and the distribution of material powder within the pellets.

4.3.1. Traditional model: Model 1

The spectral extinction coefficients of aerogel composites calculated from the traditional model are shown in Fig. 6. The measured spectral extinction coefficients of different thickness aerogel composites are very close to each other. Three samples have the same absorption peaks. The results show that silica aerogels have weak absorption within the wavelength range of 1.4–8 μm which will lead to a high radiative thermal conductivity. In order to reduce the radiative thermal conductivity, especially at elevated temperature, SiC opacifier with diameter of 3.5 μm is doped in the silica aerogel to enhance the

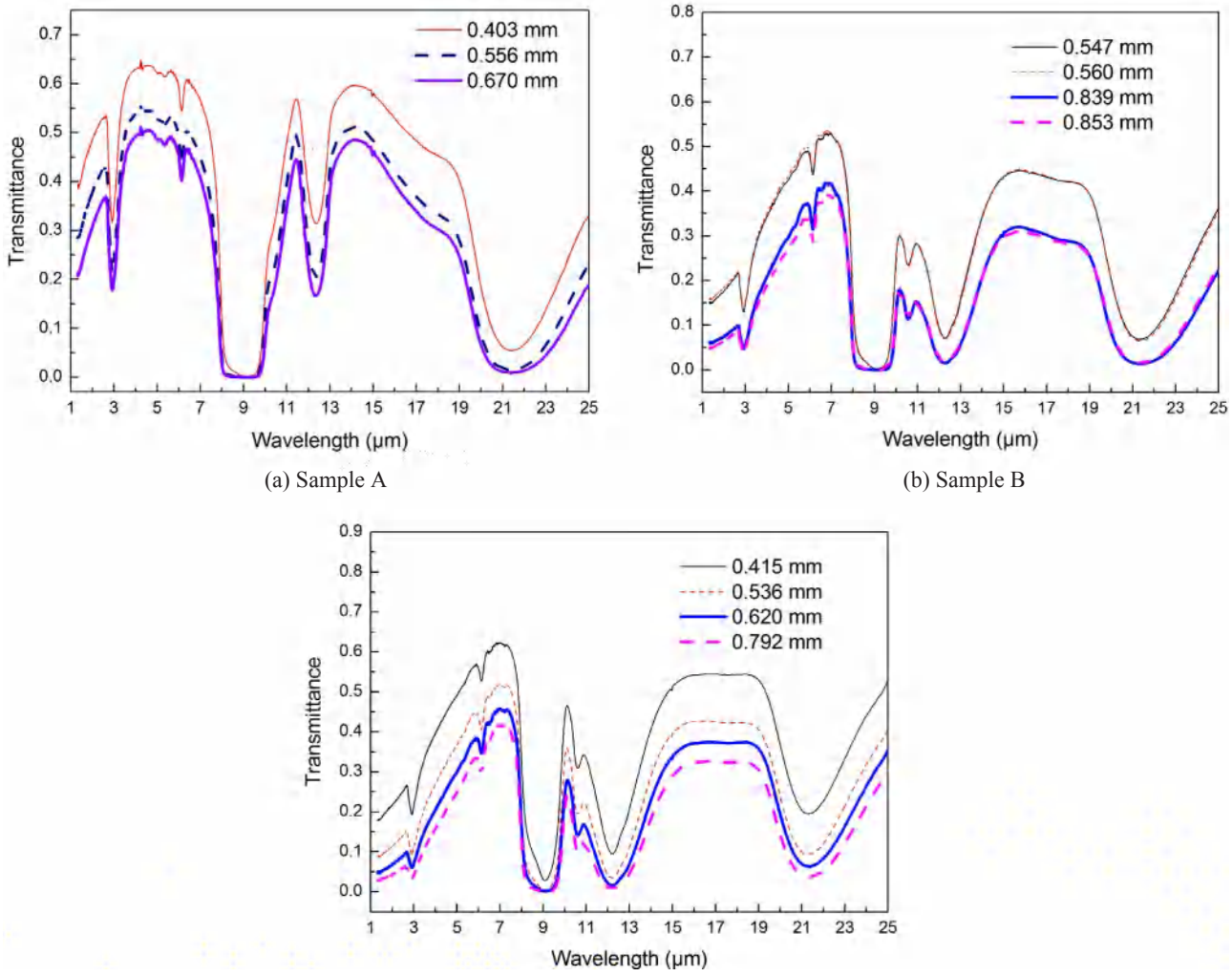

Fig. 5. Transmittances of KBr diluted silica aerogel composites: (a) Sample A, (b) Sample B, (c) Sample C.

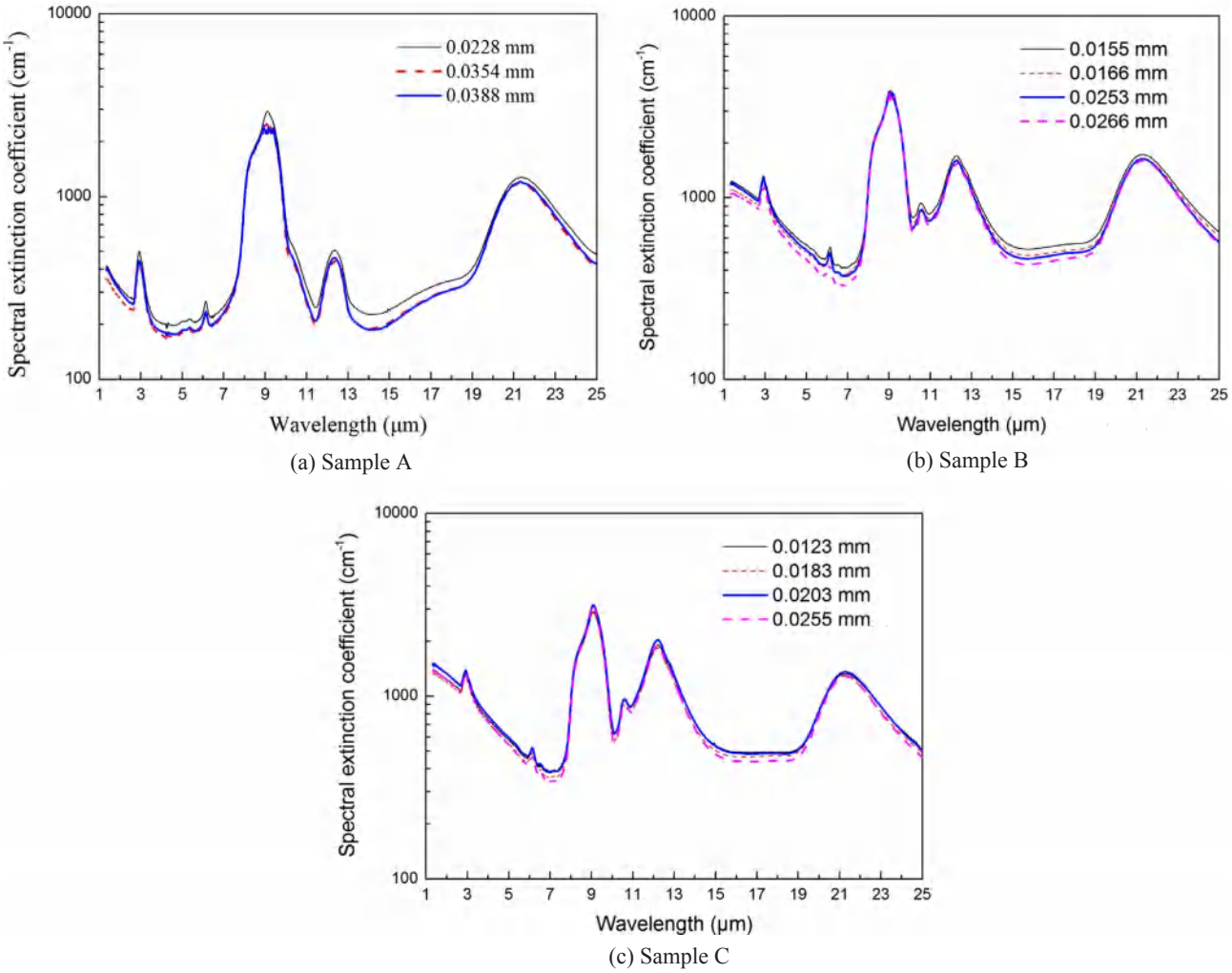

Fig. 6. Spectral extinction coefficients of aerogel composites – Model 1: (a) Sample A, (b) Sample B, (c) Sample C.

absorption within the above wavelength range. The spectral extinction coefficients measured from pellets of different thickness are similar.

4.3.2. Improved model: Model 2

In Model 2, the practical absorption of KBr is considered. The calculated results are shown in Fig. 7. Although the measured spectral extinction coefficients of KBr shown in Fig. 4 are at most 1.3% of the value of silica aerogel composite determined from Model 1 at each wavelength, the equivalent thicknesses of KBr in the diluted pellets are at least 15 times thicker than the equivalent thicknesses of silica aerogel powder. This will lead to a difference of extinction coefficient calculated by the two models for Sample A. The spectral extinction coefficient obtained from Model 2 is about 10%–20% higher than that calculated from Model 1 for wavelength shorter than 7.5 μm while the proportion is less than 9% for wavelength between 7.5–11 μm.

4.3.3. Improved model: Model 3

The reflection of the pellets in the above two models have not been taken into account which will lead to an overestimation of the extinction coefficient. The following two models are proposed to exclude the influence of reflectance. Several pellets of KBr diluted silica aerogel with same mass ratio but different thickness are measured. These pellets are prepared with the same procedures and the same facilities. Thus, the reflectance of different thickness pellets can be regarded as a constant and excluded by a least square fitting procedure. Model 3 considers the surface reflection, absorption of KBr, and silica aerogel composite powder is in series with KBr. The fitting is made for each wavelength of three kinds of samples. The spectral extinction coefficients and the fitting correlation coefficients of three samples are shown in Fig. 8. This figure clearly shows that the absorption of silica aerogel doped with opacifier is enhanced at full wavelength, especially at wavelength less than 7 μm. Sample C has a higher spectral extinction coefficient at short wavelength since it is loaded with more opacifier than Sample B. Fig. 8 also shows that the fitting correlation coefficients at different wavelength are typically higher than 0.97, which proves that this fitting method could extrude the influence of sample surface reflection.

4.3.4. Improved model: Model 4

The calculation of equivalent thickness of aerogel in the pellet from Eq. (2) essentially assumes aerogel powder is in series with KBr diluents along the through-plane direction. In practice, KBr and aerogel powder are well mixed before pressing the pellets. Aerogel powders with very low volume fraction (~6% for Sample A, ~3% for Samples B and C) in the KBr diluents are more like a random distribution. The spectral extinction coefficients of aerogel composite are calculated using the stochastic model as shown in Fig. 9. The figure also presents the fitting correlation coefficients of three samples within the full test wavelength range which are mainly higher than 0.97. It also implies that the proposed model could be used to extract the spectral extinction coefficient from the measured transmittance. Due to the strong absorption around 9 μm, the KBr diluted pellets are almost opaque at this wavelength

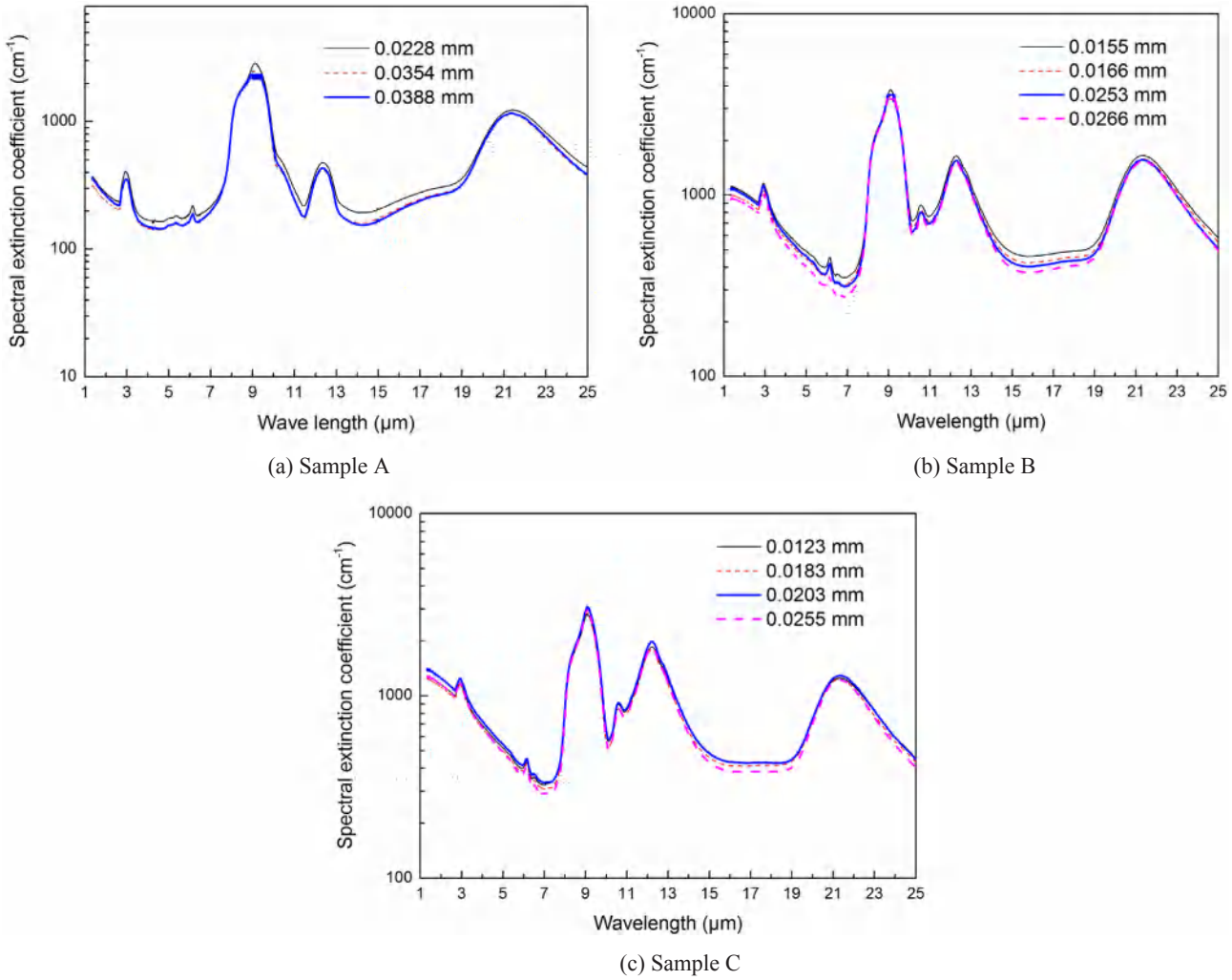

Fig. 7. Spectral extinction coefficients of aerogel composites – Model 2: (a) Sample A, (b) Sample B, (c) Sample C.

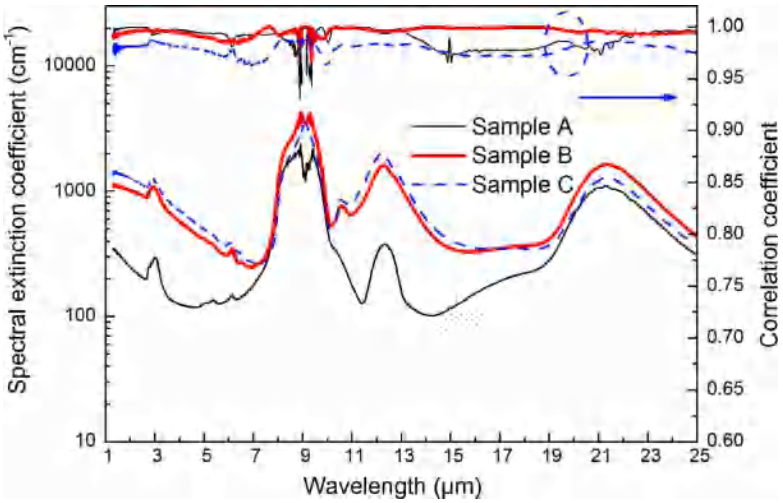

Fig. 8. Spectral extinction coefficients and correlation coefficients – Model 3.

region as shown in Fig. 5. It can then be concluded that the spectral extinction coefficient determined from Model 4 is extremely large at this wavelength region and the correlation coefficient is not high. The influence of layer thickness (corresponding to different value of m) on the extinction coefficient is compared for sample C as shown in Fig. 10. The spectral extinction coefficient has little change (< 10% except for the peaks) when the layer thickness is less than 1 μm. For the wavelength ranges from 3–8 μm where transmits most of raidation, the spectral extinction coefficient varies as much as 10%–40% for different layer thickness. It implies that the layer thickness has a modest influence on the extinction coefficient. The effect of layer thickness on the mean extinction coefficient and radiative thermal conductivity is calculated and compared in Fig. 11. The mean extinction coefficient decreases with the decrement of layer thickness while the radiative

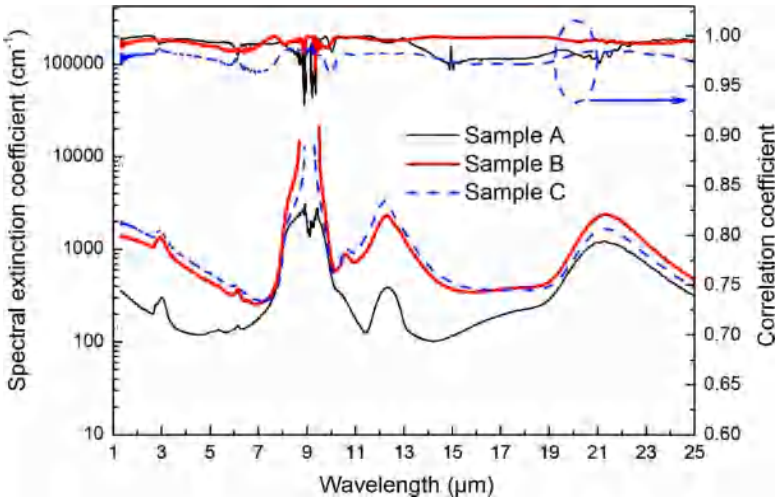

Fig. 9. Spectral extinction coefficients and correlation coefficients – Model 4.

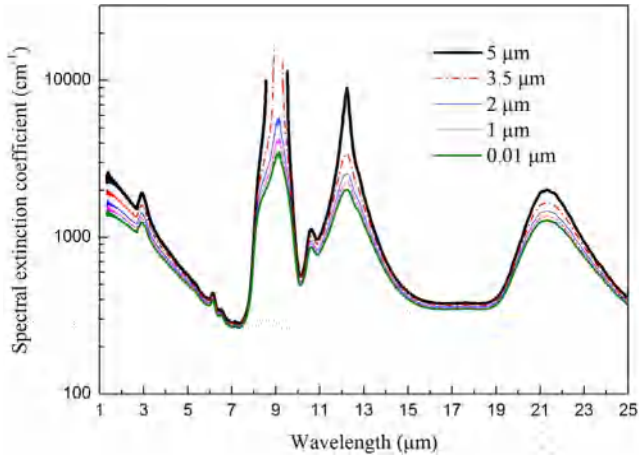

Fig. 10. Influence of layer thickness on the spectral extinction coefficient – Model 4.

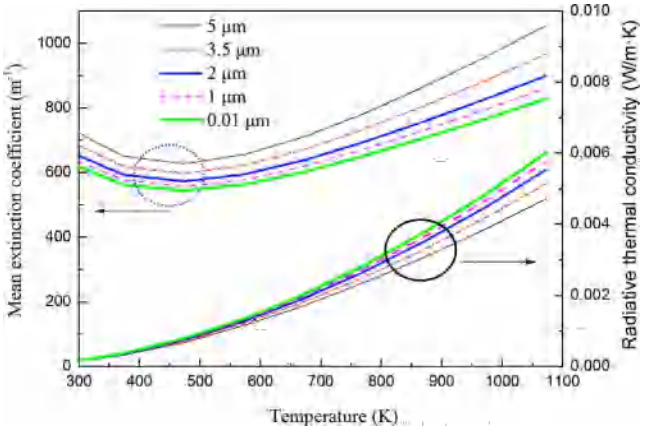

Fig. 11. Influence of layer thickness on determining the radiative properties.

thermal conductivity has the inverse variation. The difference is more pronounced at high temperature. The calculated properties remain the same (< 0.05% compared with 0.01 μm) as the layer thickness is less than 0.01 μm. Compared to the result with 0.01 μm layer thickness, the measured radiative thermal conductivity at 1073 K is 21.5% less for the layer with 5 μm thick while the proportions are 14.5%, 7.9% for the layers with thicknesses of 3.5 μm and 2 μm, respectively.

It is worth noting that the value of m in model 4 is not an arbitrary value or infinite. The silica aerogel composite with fiber and opacifier is ground with mortar and the SEM of the composite after grinding is shown in Fig. 12. Reinforced fiber and opacifers remain the same size and shape as the raw composite while the silica aerogel matrix was ground from bulk into particles with size of several microns. In the above models, the measured spectral extinction coefficient of the composites is the overall effective spectral extinction coefficient of aerogel matrix, fiber and opacifier. The size of aerogel matrix, fiber and opacifier are on the order of several microns after grinding and among these components the opacifier has much higher absorption capacity compared to the silica matrix and fiber. Therefore, the thickness of each layer is set as equal to the mean diameter of opacifier (3.5 μm) for Samples B and C, and 2 μm for Sample A (it has no opacifier and the mean diameter of the aerogel matrix is approximate to 2 μm which can be seen from the SEM) in Model 4 and then the relevant value of m in Eq. (10) can be estimated. There is a concern that the extinction properties of the aerogel can potentially change after grinding. The absorption properties of silica will remain the same irrespective of the particle size while the scattering will possibly be dependent on the size of the aerogel particles. The sizes of pores and matrix solid structure of the aerogel composite studied here are on the magnitude of several nanometer or dozens of nanometer. After grinding, the diameter of the aerogel matrix powder (~several microns) is at least 100 times larger than the size of pores and matrix structure which can be regarded as a homogeneous medium when compared to the nano-porous pores and structures. The shape and size of fiber and opacifier remain unchanged during the grinding process. In addition, the doping of opacifier attenuates more radiation as shown in Fig. 8. Thus the size effect of aerogel matrix particles on scattering is neglected in this study.

4.3.5. Comparison of different models

The spectral extinction coefficients calculated from four models are compared in Fig. 13. The same spectral trend can be obtained from different models for the same material. The extinction coefficients predicted by different models are not identical. Large differences exist at 9.1 μm, 12.3 μm and 21.2 μm because the transmittances at these wavelengths are miniscule, which will bring in a large uncertainty. However, the absolute value of spectral extinction coefficient at this wavelength region is not essential. Because most of the thermal radiation in aerogel composite is transmitted via the near-infrared and mid-infrared light when used as thermal insulating material at high temperature according to Plank's law. In addition, silica aerogel composites have a relatively low extinction coefficient at the near-infrared and mid-infrared regions. Therefore, the low extinction coefficient in the short-wavelength region is the major contributor to radiative heat transfer. Take Sample A as an example, for temperature less than 1000 K the Rosseland mean extinction coefficient determined from

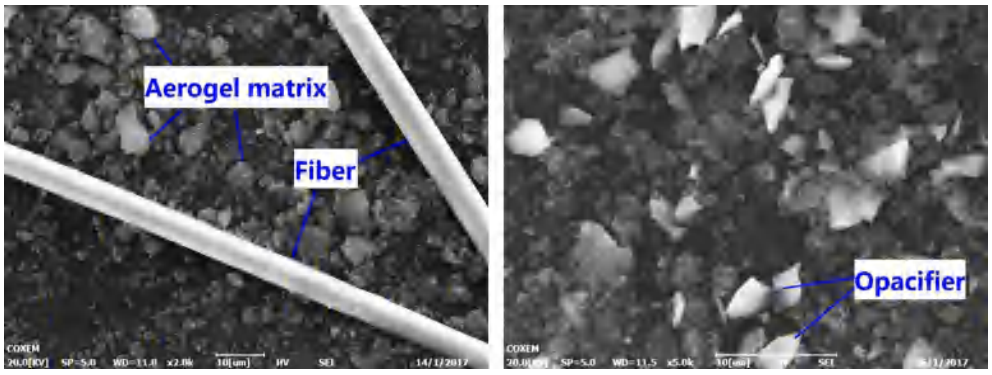

Fig. 12. SEM of aerogel composite after grinding.

Model 2 is 13%–15% less than that determined from Model 1, 15%–25% less than that determined from Model 2 for Model 3 while only 1.3%–1.9% higher than that determined from Model 3 for Model 4. It proves that in an FTIR test the measured mean extinction coefficient will be overestimated if neglecting the practical absorption of KBr diluents and the sample surface reflection. In the near-infrared and mid-infrared regions, the extinction coefficients determined from Model 3 and Model 4 are almost identical to each other which implies that the geometric arrangement has little influence on the result.

4.4. Radiative thermal conductivity

With the measured spectral extinction coefficients of silica aerogel composites from different models, the Rosseland mean extinction coefficient can be obtained with values at least higher than 70 cm^{-1} for different models and different materials. It implies that the optical thickness of such kind of material with thickness of 1 cm is at least larger than 70 which proves that its radiative thermal conductivity can be well predicted by the Rosseland model [32] using Eq. (11).

In the calculation, the extinction coefficient determined from four different models are adopted and compared. The radiative thermal

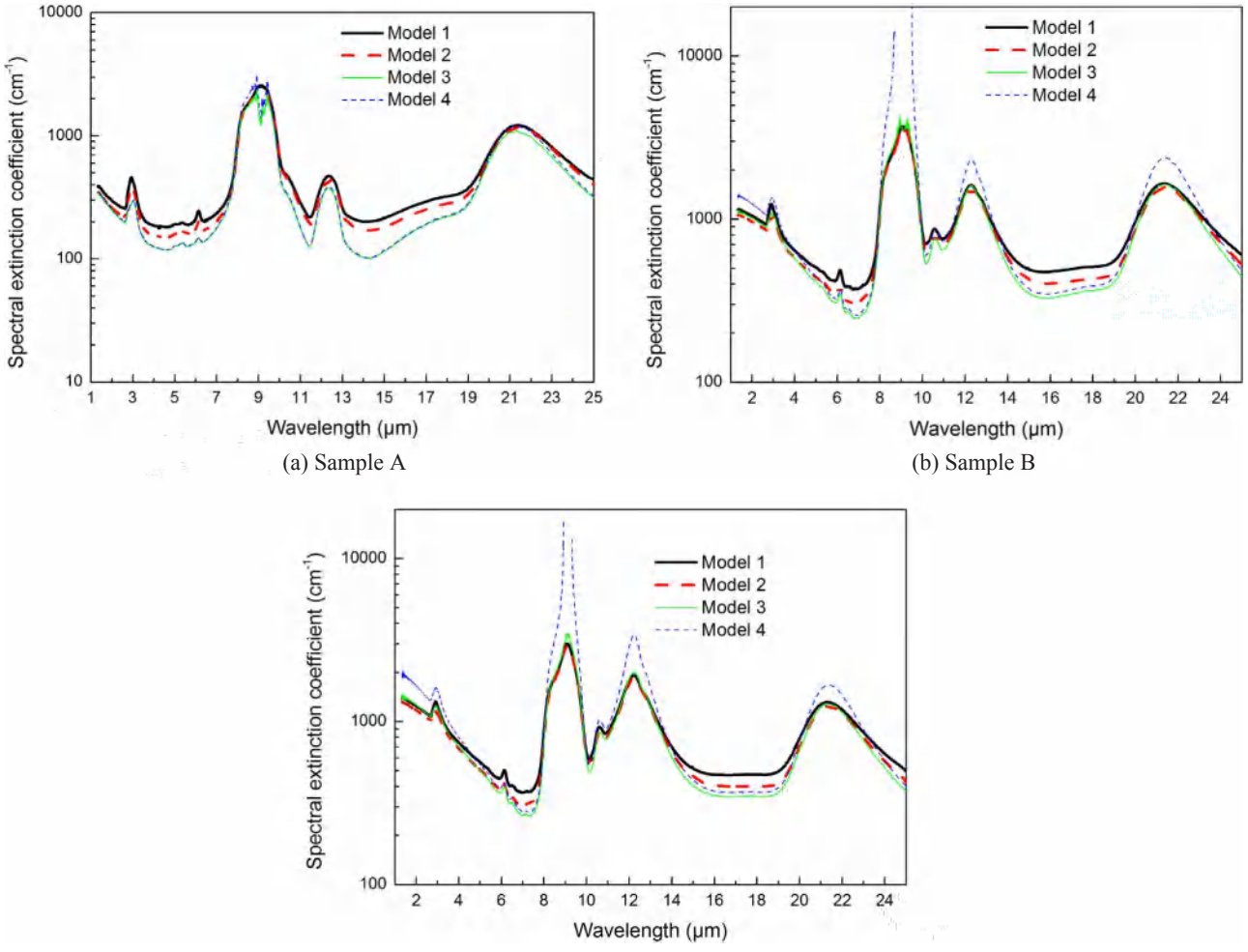

Fig. 13. Comparisons of extinction coefficients determined from different models: (a) Sample A, (b) Sample B, (c) Sample C.

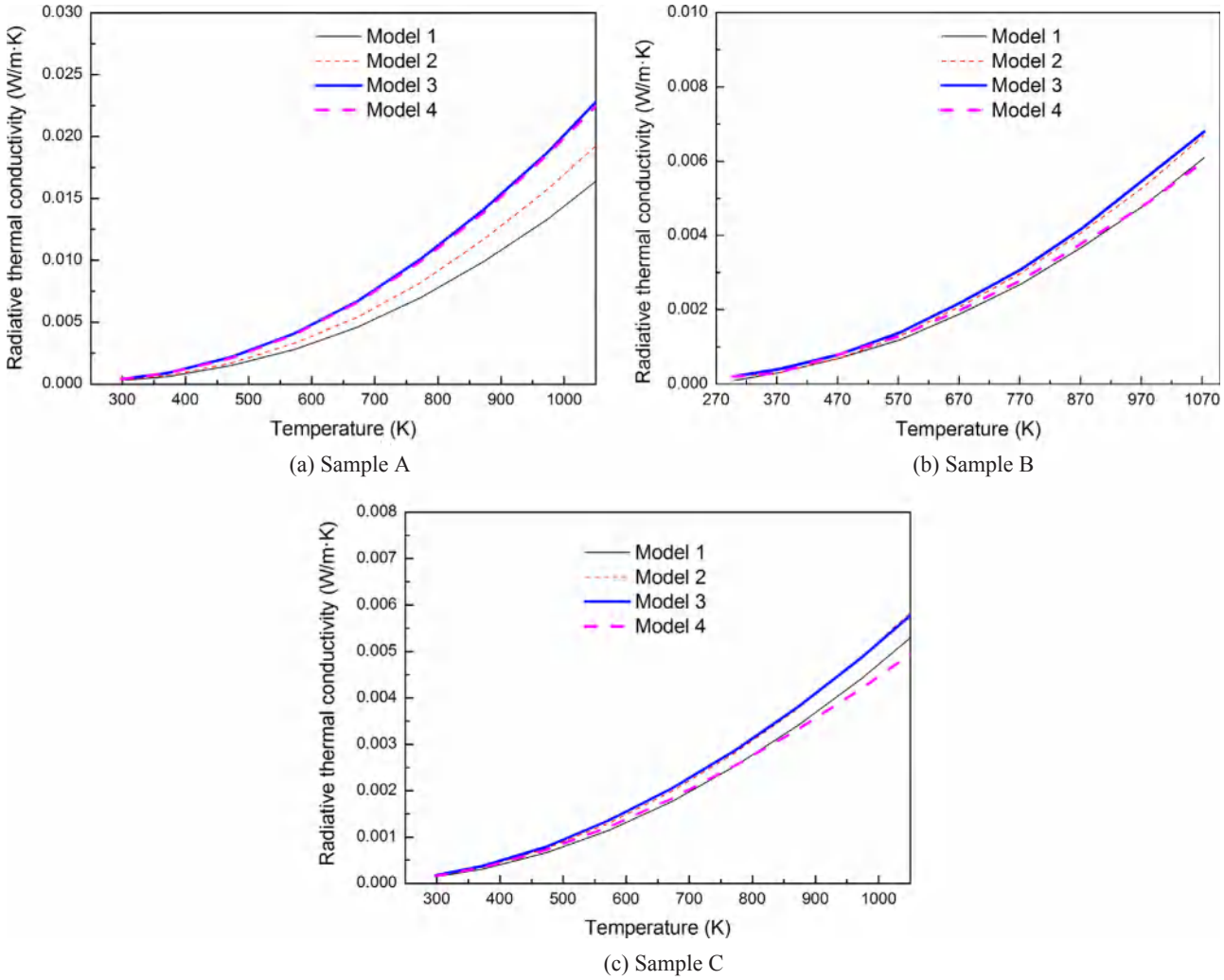

Fig. 14. Radiative thermal conductivity obtained from different models: (a) Sample A, (b) Sample B, (c) Sample C.

conductivity of different materials is shown in Fig. 14. The extinction coefficients determined by the above four models are different and thus lead to a different radiative thermal conductivity at high temperature, especially for Sample A without doping opacifier. SiC opacifier is loaded in Samples B and C, thus they have lower radiative thermal conductivity than Sample A. Sample C has a lower radiative thermal conductivity than Sample B since it loaded more opacifier. The difference of extinction coefficient and radiative thermal conductivity obtained from different models for the same materials proves that the assumptions in traditional model indeed introduce some uncertainty. The models proposed in this study could overcome these drawbacks of traditional model.

5. Conclusion

This study presents improved models of extracting spectral extinction coefficients from the transmittance of KBr diluted materials measured by FTIR. Compared with the traditional model, these models take into account the practical transparency of KBr diluents, the sample surface reflection, and the distribution of measured material in the KBr diluents. These improved models overcome the drawbacks or assumptions of the previous model and thus have a better accuracy on determining the extinction coefficient from the measured transmittance. The practical absorption of KBr diluents and sample surface reflection cannot be neglected for materials with high transparency. The comparison for Sample A at temperature less than 1000 K found that the measured mean extinction coefficient will be overestimated if neglecting the practical absorption of KBr diluents (about 15%–18%) and the sample surface reflection (about 18%–33%) in the practical FTIR measurement. The geometric arrangement has less effect on determining the extinction coefficient in the near-infrared and mid-infrared regions.

With the extinction coefficient determined from the proposed models, the radiative thermal conductivity of silica aerogel composites can be predicted by the Rosseland model since these materials are optically thick mediums in practical applications. The measured radiative thermal conductivity obtained from different models also has difference since it is reciprocal to the Rosseland mean extinction coefficient and proportional to temperature to the third power. The present study provides an effective method of predicting radiative thermal conductivity of silica aerogels doped with reinforced fiber and opacifier via extracting the extinction coefficient from an FTIR transmittance measurement. The models developed in this study are also suitable to the materials that need to be diluted when measuring extinction coefficient with FTIR.

Acknowledgements

The authors would like to thank the supports from National Natural Science Foundation of China (Grant No. 51606143), China Postdoctoral Science Foundation (Grant No. 2016M602814) and Shaanxi Province Postdoctoral Science Foundation (Grant No. 2016BSHEDZZ133).

References

[1] J.-J. Zhao, Y.-Y. Duan, X.-D. Wang, B.-X. Wang, Radiative properties and heat transfer characteristics of fiber-loaded silica aerogel composites for thermal insulation, Int. J. Heat Mass Transf. 55 (2012) 5196–5204.

[2] J.-J. Zhao, Y.-Y. Duan, X.-D. Wang, X.-R. Zhang, Y.-H. Han, Y.-B. Gao, Z.-H. Lv, H.-T. Yu, B.-X. Wang, Optical and radiative properties of infrared opacifier particles loaded in silica aerogels for high temperature thermal insulation, Int. J. Therm. Sci. 70 (2013) 54–64.

[3] G. Wei, Y. Liu, X. Zhang, X. Du, Radiative heat transfer study on silica aerogel and its composite insulation materials, J. Non-Cryst. Solids 362 (2013) 231–236.

[4] X.-D. Wang, D. Sun, Y.-Y. Duan, Z.-J. Hu, Radiative characteristics of opacifier-loaded silica aerogel composites, J. Non-Cryst. Solids 375 (2013) 31–39.

[5] S. Zeng, A. Hunt, W. Cao, R. Greif, Approximate formulation for coupled conduction and radiation through a medium with arbitrary optical thickness, ASME J. Heat Transf. 117 (1995) 797–799.

[6] S. De Iuliis, N. Chaumeix, M. Idir, C.-E. Paillard, Scattering/extinction measurements of soot formation in a shock tube, Exp. Thermal Fluid Sci. 32 (2008) 1354–1362.

[7] W. An, Q. Zhu, T. Zhu, N. Gao, Radiative properties of gold nanorod solutions and its temperature distribution under laser irradiation: experimental investigation, Exp. Thermal Fluid Sci. 44 (2013) 409–418.

[8] A. Menbari, A.A. Alemrajabi, Y. Ghayeb, Investigation on the stability, viscosity and extinction coefficient of $CuO–Al_2O_3$/water binary mixture nanofluid, Exp. Thermal Fluid Sci. 74 (2016) 122–129.

[9] H. Liu, X.-L. Xia, Q. Ai, X.-Q. Xie, C. Sun, Experimental investigations on temperature-dependent effective thermal conductivity of nanoporous silica aerogel composite, Exp. Thermal Fluid Sci. 84 (2017) 67–77.

[10] T. Xie, Y.-L. He, Z.-J. Hu, Theoretical study on thermal conductivities of silica aerogel composite insulating material, Int. J. Heat Mass Transf. 58 (2013) 540–552.

[11] Y.-L. He, T. Xie, Advances of thermal conductivity models of nanoscale silica aerogel insulation material, Appl. Therm. Eng. 81 (2015) 28–50.

[12] J.-J. Zhao, Y.-Y. Duan, X.-D. Wang, B.-X. Wang, An analytical model for combined radiative and conductive heat transfer in fiber-loaded silica aerogels, J. Non-Cryst. Solids 358 (2012) 1303–1312.

[13] J.-J. Zhao, Y.-Y. Duan, X.-D. Wang, B.-X. Wang, A 3-D numerical heat transfer model for silica aerogels based on the porous secondary nanoparticle aggregate structure, J. Non-Cryst. Solids 358 (2012) 1287–1297.

[14] J.-J. Zhao, Y.-Y. Duan, X.-D. Wang, B.-X. Wang, Experimental and analytical analyses of the thermal conductivities and high-temperature characteristics of silica aerogels based on microstructures, J. Phys. D Appl. Phys. 46 (2013) 015304.

[15] C. Bi, G.-H. Tang, Z.-J. Hu, H.-L. Yang, J.-N. Li, Coupling model for heat transfer between solid and gas phases in aerogel and experimental investigation, Int. J. Heat Mass Transf. 79 (2014) 126–136.

[16] D. Dan, H. Zhang, W.-Q. Tao, Effective structure of aerogels and decomposed contributions of its thermal conductivity, Appl. Therm. Eng. 72 (2014) 2–9.

[17] W.-Z. Fang, H. Zhang, L. Chen, W.-Q. Tao, Numerical predictions of thermal conductivities for the silica aerogel and its composites, Appl. Therm. Eng. 115 (2017) 1277–1286.

[18] X. Lu, M. Arduini-Schuster, J. Kuhn, O. Nilsson, J. Fricke, R. Pekala, Thermal conductivity of monolithic organic aerogels, Science 255 (1992) 971–972.

[19] S. Zeng, A. Hunt, R. Greif, Geometric structure and thermal conductivity of porous medium silica aerogel, ASME J. Heat Transf. 117 (1995) 1055–1058.

[20] G.-S. Wei, L.-X. Wang, C. Xu, X.-Z. Du, Y.-P. Yang, Thermal conductivity investigations of granular and powdered silica aerogels at different temperatures and pressures, Energy Build. 118 (2016) 226–231.

[21] T. Xie, Y.-L. He, Heat transfer characteristics of silica aerogel composite materials: structure reconstruction and numerical modeling, Int. J. Heat Mass Transf. 95 (2016) 621–635.

[22] S. Zeng, R. Greif, P. Stevens, M. Ayers, A. Hunt, Effective optical constants n and κ and extinction coefficient of silica aerogel, J. Mater. Res. 11 (1996) 687–693.

[23] J. Kuhn, F. Schwertfeger, M. Arduini-Schuster, J. Fricke, U. Schubert, Structural investigations of pyrolyzed organically modified SiO_2 aerogels, J. Non-Cryst. Solids 186 (1995) 184–190.

[24] L. Zhao, S. Yang, B. Bhatia, E. Strobach, E.N. Wang, Modeling silica aerogel optical performance by determining its radiative properties, AIP Adv. 6 (2016) 025123.

[25] T.-R. Fu, J.-Q. Tang, K. Chen, F. Zhang, Determination of scattering and absorption coefficients of porous silica aerogel composites, ASME J. Heat Transf. 138 (2016) 032702.

[26] E. Cohen, L. Glicksman, Thermal properties of silica aerogel formula, ASME J. Heat Transf. 137 (2015) 081601.

[27] S. Lallich, F. Enguehard, D. Baillis, Experimental determination and modeling of the radiative properties of silica nanoporous matrices, ASME J. Heat Transf. 131 (2009) 082701.

[28] G.-S. Wei, Y.-S. Liu, X.-X. Zhang, F. Yu, X.-Z. Du, Thermal conductivities study on silica aerogel and its composite insulation materials, Int. J. Heat Mass Transf. 54 (2011) 2355–2366.

[29] G.-H. Tang, C. Bi, Y. Zhao, W.-Q. Tao, Thermal transport in nano-porous insulation of aerogel: factors, models and outlook, Energy 90 (2015) 701–721.

[30] Z.-J. Xu, Z.-L. Lu, L.-H. Gan, Z.-X. Hao, L.-W. Chen, Study of phase transition in SiO_2 aerogel balls during the heat treatment, J. Syn. Cryst. 35 (2006) 1176–1179.

[31] H. Chen, Z. Sun, J. Shao, Investigation on FT-IR spectroscopy for eight different sources of SiO_2, Bull. Chin. Ceram. Soc. 30 (2011) 934–937.

[32] H. Zhang, Y.-M. Li, W.-Q. Tao, Effect of radiative heat transfer on determining thermal conductivity of semi-transparent materials using transient plane source method, Appl. Therm. Eng. 114 (2017) 337–345.